Critical coverage for strain-induced formation of InAs quantum dots

Ch. Heyn*
Institut für Angewandte Physik und Zentrum für Mikrostrukturforschung, Jungiusstraße 11, D-20355 Hamburg, Germany
(Received 14 December 2000; revised manuscript received 4 May 2001; published 3 October 2001)

The critical coverage θ_C for the strain-induced transformation of initial two-dimensional (2D) InAs or InGaAs growth islands into quantum-dot-like three-dimensional (3D) islands is studied with *in situ* electron diffraction under variation of the flux F, temperature T, and lattice mismatch δ given by the Ga content in InGaAs films. The experimental data are compared to calculations based on a kinetic rate model with layer dependent strain energy inside the islands. With the growth model, the lateral size distribution and the height of the islands is calculated, as well as θ_C. Good agreement between experiments and rate equation results is obtained for the influence of δ and F on θ_C, whereas the T dependencies show a contradictory behavior. This is explained by a temperature-dependent intermixing between the deposited In and Ga from the substrate. Considering this effect in the calculations allows a determination of the temperature-dependent Ga content. Additional calculation results point out that the island diameter shrinks during the 2D to 3D transition and that the island shape is not in equilibrium during growth.

DOI: 10.1103/PhysRevB.64.165306 PACS number(s): 61.14.Hg, 68.35.Rh, 61.46.+w, 81.15.Hi

I. INTRODUCTION

The application of self-assembling mechanisms has been established as a powerful method for the fabrication of nanometer-sized structures without the need of lithographic steps.[1] A prominent example is three-dimensional (3D) quantum-dot-like islands of InAs or InGaAs on GaAs substrates grown with molecular-beam epitaxy (MBE) (Refs. 2–4) or metal organic chemical vapor deposition (MOCVD) (Refs. 5–7) in the so-called Stranski-Krastanov (SK) mode. The driving force for this self-assembling mechanism is the strain inside the deposited film which is due to the lattice mismatch between the substrate and the deposit. During SK growth, first a thin wetting layer (WL) is formed. At a critical coverage θ_C, the accommodated strain energy initiates the transition from a flat two-dimensional (2D) surface morphology into 3D islands. One main advantage of these coherently strained SK islands is their uniform size distribution[2] when compared, e.g., with islands grown in the Volmer-Weber mode. Many approaches to model the SK growth mechanisms were presented mainly by referring equilibrium arguments[8,9] or the kinetics of adatoms on the surface.[10–13]

Strain-driven migration of atoms from the edges on top of initial 2D growth islands is responsible for their conversion into 3D ones. The central parameter for this conversion is the lateral binding energy E_{isl} between adatoms and island edges which controls the mass transport on the island top. Most of the recent kinetic SK growth models[10–13] consider only the influence of the island radius r on E_{isl}, often in the form[10–12] $E_{isl}=E_0\ln(r)/r$, with the model parameter E_0. The model presented here discusses a different approach for the effect of strain. It is assumed that atoms in upper layers of the island influence E_{isl} as well. In other words, the influence of strain is related to the island volume rather than to its diameter. In particular, E_{isl} is approximated by a two-spring model that allows the quantitative inclusion of the lattice mismatch. The calculation results are linked to experimental data taken with *in situ* reflection high-energy electron diffraction (RHEED) for variations of the growth parameters.

II. EXPERIMENTAL SETUP

The samples are grown in a solid-source MBE machine equipped with a 12-keV RHEED system. Starting from planar (001) GaAs substrates, first a GaAs buffer is grown at 600 °C in order to smooth the surface. The resulting surface morphology is controlled with *in situ* RHEED. A clear 2×4 reconstruction with diffraction patterns lying on a Laue circle in $[\bar{1}10]$ azimuth indicates a smooth GaAs surface. For growth of the InAs quantum dots the temperature is reduced down to $T=420$–530 °C resulting in a change of the GaAs surface reconstruction to $c(4\times4)$. A typical RHEED pattern is shown in Fig. 1(a).

$In_{1-x}Ga_xAs$ deposition is performed with growth rates $F=0.02$–0.3 monolayer/s, the Ga content x is varied from 0 up to 70%, and the As_4 flux corresponds to a flux gauge reading of 10^{-5} Torr. The respective growth rates are determined as is described in Ref. 14. Directly after InGaAs deposition is started, the surface reconstruction changes again [Fig. 1(b)]. As for the GaAs buffer surface, the RHEED pattern at low InGaAs coverages is due to diffraction from flat two-dimensional surface features. When the coverage θ exceeds a critical value θ_C, the RHEED pattern changes qualitatively. Now the peaks represent the reciprocal InGaAs lattice and originate from transmission diffraction through three-dimensional quantum-dot-like islands [Fig. 1(c)]. We note that after transition into the bulklike reflection typical intensity tails so-called chevrons[15] are attached to the RHEED spots that are directly associated to the dot formation.

The critical coverage θ_C for 2D to 3D transition is precisely determined from the RHEED signals according to Ref. 14. An example for the intensity evolution of a 2D growth related spot for $\theta<\theta_C$ and of a 3D spot for $\theta>\theta_C$ is shown in Fig. 1. The respective RHEED spots marked by arrows are shown in Figs. 1(a)–1(c). In addition, some samples are investigated with atomic force microscopy (AFM) for the determination of island density, height, and lateral size.[16] After growth, these samples are rapidly cooled down by switching

 ©2001 The American Physical Society

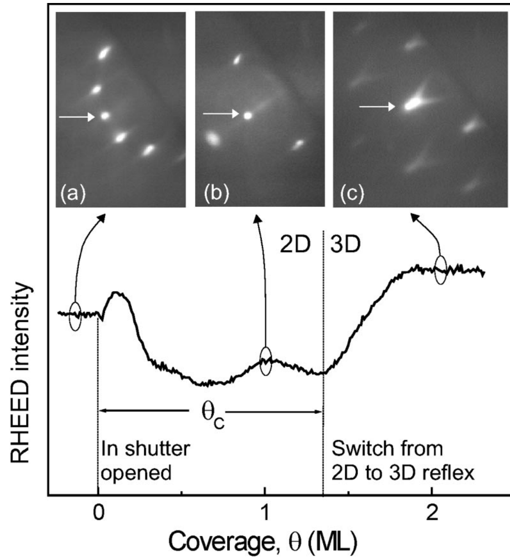

FIG. 1. Time evolution of the intensity of 2D and 3D growth related reflexes together with corresponding RHEED patterns of GaAs and InAs surfaces. (a) Flat GaAs surface at 420 °C in $[\bar{1}10]$ azimuth, the arrow indicates the 2D-type reflex that is used for the measurement of the time-dependent intensity, (b) after deposition of 1.0-ML InAs, the arrow indicates the 2D reflex; (c) transmission diffraction and appearance of chevrons after deposition of 2.0-ML InAs, the arrow indicates the 3D reflex used for the time-dependent measurements. The 3D reflex appears at a critical coverage θ_C.

off the heater in order to preserve the as-grown surface morphology.

III. GROWTH MODEL FOR STRAIN-INDUCED 3D ISLANDS

The rate equations based growth model presented here accounts for kinetic processes of single atoms on the surface. After growth is started, indium atoms impinge with flux F on an initially flat GaAs surface. It is assumed that arsenic is incorporated only via reaction with indium on the surface. Excessive arsenic will desorb. Therefore, at a sufficient As_4 flux, a stoichiometric InAs layer will be formed automatically. For simplification, arsenic incorporation mechanisms are not included in the model. The mobile adatoms migrate thermally activated on the surface. Collisions between migrating adatoms result in nucleation of initial 2D growth islands with approximately monolayer (ML) height. These islands grow laterally by attachment of additional adatoms and vertically by direct hits from the vapor beam as well as by atoms hopping from island edges on top of the islands. Once the island diameter is large enough, the strain induced by the lattice mismatch between the substrate and the deposit significantly enhances the latter process resulting in a strong increase of the island height.

A. Structural aspects

In the model, three different layer types of the InAs deposit are distinguished: the wetting layer, the active layer, and the upper layers at higher levels (Fig. 2). The lowest

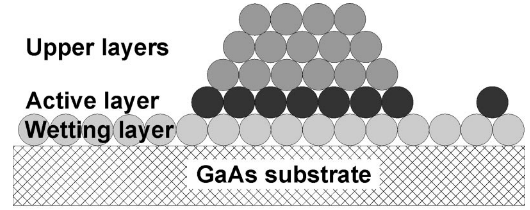

FIG. 2. Schematic drawing of the different layers relevant for the growth model. Details are given in the text.

InAs layer directly on top of the GaAs substrate is the so-called wetting layer. Characteristic for this layer is a chemical attraction between indium and gallium which hinders upward migration of In atoms from the wetting layer into higher levels. The evolution of the wetting layer coverage θ_W with deposition time t is taken as $d\theta_W/dt = F(1-\theta_W)$. Once θ_W is large enough, atoms will impinge on top of the wetting layer as well and nucleate islands there. The second layer on top of the wetting layer is denoted as active layer. In contrast to those from the wetting layer, atoms from the active layer can migrate to higher levels. The kinetic behavior of atoms in the active layer is thus responsible for island nucleation and shape evolution. In this picture, an island consists of a base with s atoms located in the active layer and u_s/n_s atoms on top of this base in the upper layers, with the density n_s of islands with base area s and the density u_s of atoms in the upper layers of all islands with base area s. In all, an island consists of $V_s = s + u_s/n_s$ atoms. Furthermore, we assume that islands are shaped as truncated square-based pyramids with base length $s^{0.5}$ and an angle[17] of 26° between the side facets and the substrate. This allows the calculation of the island height h_s once s and V_s are known.

The strain induced by the difference of the lattice constants a_{GaAs} and a_{InAs} between the GaAs substrate and the InAs deposit is the driving force for the transition of initially 2D growth islands to 3D quantum-dot-like islands. Regarding the mass transport of atoms from island perimeter sites on top of the islands, the activity of atoms at island edges is the essential parameter. According to previous models[10,11,18] we assume that the strain influences the lateral binding energy E_{isl} between adatoms and edges of the island base. In the present model, bonds between atoms within the island base are regarded to act similar to a spring. Due to the lattice mismatch the spring is compressed and the strain energy within the base layer is $c_B\delta^2 s$, where $c_B = (1/2)\zeta_B a_{GaAs}^2$, ζ_B is equivalent to a spring constant, and $\delta = (a_{InAs} - a_{GaAs})/a_{GaAs}$ is the lattice mismatch. A second spring derives from atoms on top of the island in the upper layers with strain energy $c_U\delta^2(u_s/n_s)$, and the constant c_U. Both springs together yield a repulsive force for the outermost atoms at the island base and reduce the lateral binding energy to $E_{isl} = E_0 - [c_B s + c_U(u_s/n_s)]\delta^2$, with the model parameter E_0.

B. Rate equations

Islands with base area s grow laterally by adatom attachment with rate $R_{A,s} = n_1 \nu_{free} n_s \sigma_s$, where n_1 and ν_{free} are

the density and the hopping frequency of a free mobile adatom, respectively. The capture numbers σ_s consider the spatial distribution of the monomers around the islands and are calculated according to the self-consistent approach of Bales *et al.*[19,20] The hopping frequency is $\nu_{free} = \nu_0 \exp(-E_{free}/k_B T)$, where $\nu_0 = (2k_B T)/h$ is taken as vibrational frequency, k_B is Boltzmann's constant, T is the substrate temperature, h is Planck's constant, and E_{free} is the energy barrier for surface diffusion of a free adatom. Atoms escape from islands with rate[10,20] $R_{D,s} = (n_s \omega_s \sigma_{s-1})/[2\pi(s-1)^{0.5}]$, where $\omega_s = \nu_{isl}\chi_D s^{0.5}$ is the adatom detachment rate,[21] $\nu_{isl} = \nu_0 \exp[(-E_{free} - E_{isl})/k_B T]$ is the hopping frequency of an adatom at an island edge, and $\chi_D = 0.25\chi_D = 0.25 + 0.5/(s-1)^{0.5}$ is the island size-dependent probability that a hopping atom at an island edge will detach. The distinction between $R_{D,s}$ and ω_s reflects the fact that a detaching atom may be recaptured from the island.[20] In order to include the effect of strain, we refer to the two-spring approximation for E_{isl} described above. Atoms hop upwards from perimeter sites on top of islands with base area s with rate $R_{T,s} = n_s \nu_{isl} 0.25 s^{0.5}(1 - V_s/V_P)$, where V_P is the volume of a pyramid with base length $s^{0.5}$ and an angle of 26° between the side facets and the substrate. Downward migration is neglected in this model.

To describe the evolution of the monomer density n_1 and of the density n_s of islands with base area s, we expand the well-known set of coupled rate equations for 2D nucleation[19–22] by the rate R_T and the wetting layer coverage:

$$\frac{d}{dt}n_1 = F\theta_W\left(1 - n_1 - \sum_{s>1} s n_s\right) - 2R_{A,1} - \sum_{s>1} R_{A,s} + 2R_{D,2} + \sum_{s>2} R_{D,s} + R_{T,2}, \tag{1}$$

$$\frac{d}{dt}n_s = -(R_{A,s} + R_{D,s} + R_{T,s}) + R_{D,s+1} + R_{T,s+1} + R_{A,s-1}. \tag{2}$$

The density of atoms in the upper layers on top of all islands with base area s follows:

$$\frac{d}{dt}u_s = F s n_s + R_{T,s+1} - (u_s/n_s)(R_{A,s} + R_{D,s} + R_{T,s}) + (u_{s+1}/n_{s+1})(R_{D,s+1} + R_{T,s+1}) + (u_{s-1}/n_{s-1}) \times (R_{A,s-1}). \tag{3}$$

Equation (3) reflects that atoms hopping from the island edge on the island top yield two modifications for the island shape. First the size s of the island base area is reduced and second the density of atoms on top of the island is increased. In contrast to this, attachment and detachment processes modify only the value of s. Direct hits of impinging atoms on top of the islands are also considered but the effect is rather small in comparison to the mass transfer from island edges.

The set of $2s_{max}$ coupled rate equations is solved iteratively and allows us to calculate the size dependence of the island density and of the island height h_s (the maximum island size s_{max} up to 10^4 depends on the parameters). Three growth parameters are included in the model: the growth temperature T, the flux F, and the lattice mismatch δ. In addition, four model parameters are used: the surface diffusion barrier E_{free}, and the parameters related to the lateral binding energy in our two-spring approximation, that are E_0, c_B, and c_U.

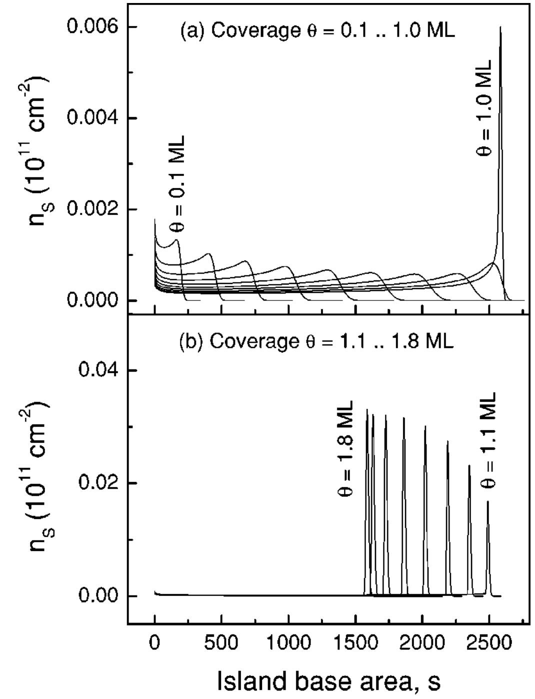

FIG. 3. Calculated island size distribution at different coverages θ in steps of 0.1 ML. (a) $\theta = 0.1$–1.0 ML's and (b) $\theta = 1.1$–1.8 ML. The growth parameters are $T = 420$ °C, $F = 0.1$ ML/s, and $\delta = 7.26\%$. The calculation parameters are identical with parameter set A as is defined in the text.

IV. RESULTS AND DISCUSSION

This section discusses rate equation results and links these to AFM and RHEED data. In subsection A the general behavior of the island density and shape is studied and the growth model is parametrized for the InAs on GaAs system. Subsection B presents RHEED data for the growth parameter dependence of θ_C and corresponding calculation results.

A. Evolution of the island shape

Examples of the island size distribution n_s at different coverages θ calculated with the rate model are plotted in Fig. 3. The growth parameters are $T = 420$ °C, $F = 0.1$ ML/s, and $\delta = 7.26\%$ representing InAs on GaAs. The model parameters agree with the parameter set A as will be defined below. At coverages smaller than 0.9 ML [Fig. 3(a)] the average island size increases with θ and the size distribution is broad which is a typical behavior of nucleation in layer-by-layer mode.[19] Importantly, the size distribution becomes narrow at coverages $\theta > 0.9$ ML. This indicates a deviation from con-

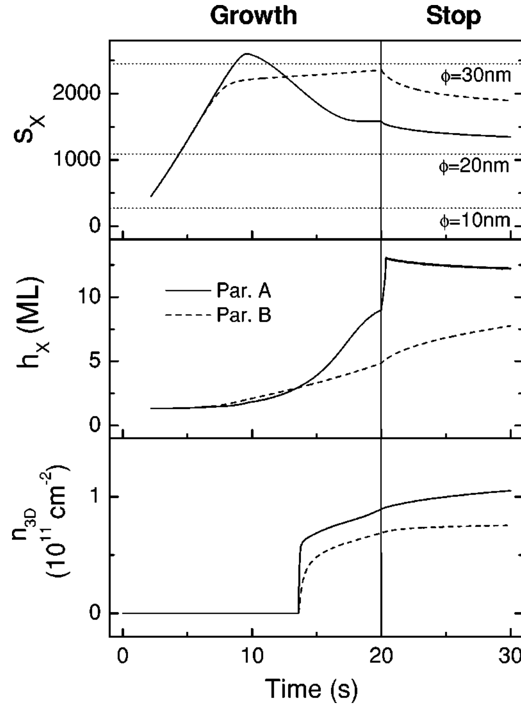

FIG. 4. Calculated time evolution of the island size s_x at which the island density is maximal, the height h_x of an island with size s_x, and the density n_{3D} of 3D islands. Calculations are performed with parameter sets A and B, the growth parameters are as in Fig. 3. The dotted lines in the upper panel are guides for the eye and represent different island diameters ϕ in nm. Growth is stopped after 20 s deposition corresponding to $\theta = 2.0$ ML's. The behavior during the following 10-s surface recovery is plotted as well.

ventional layer-by-layer growth and is a clear sign for the influence of strain. Experimental observations[2] show a very uniform size for 3D islands as well. For $\theta > 1.0$ ML [Fig. 3(b)] the situation changes qualitatively. Now, the average island size decreases with coverage. The island size distribution remains narrow.

The evolution of the island size s_x at the maximum of n_s is plotted in Fig. 4 together with the height h_x of the islands with base area s_x. Two parameter sets are discussed in parallel to study the influence of the strain in the bulk of the islands. Parameter set A represents a layer dependent strain energy inside the islands whereas parameter set B considers only the strain in the island base. Details of the parametrization are described below. Four regimes are distinguished for the island shape evolution: the 2D growth regime, the transition regime, the 3D growth regime, and the saturation regime. In the 2D growth regime at low coverages up to 0.9 ML the effect of strain is negligible. Here s_x increases nearly linear with θ, islands are approximately one monolayer high, and the island height increases only smoothly by direct hits on islands top. Once s_x is large enough, the influence of the strain becomes significant. In this transition regime, the lateral binding energy E_{isl} becomes smaller which increases the detachment rate R_D as well as the mass transport on top of the islands with rate R_T. The latter yields an increase of the density u_s, and, in the case of parameter set A, a further reduction of E_{isl}. As a result, the island height strongly increases at the expense of the shrinking island diameter. In contrast to this behavior, parameter set B yields a saturated island diameter and only a smooth increase of h_x. At $\theta > 1.8$ ML, s_x calculated with parameter set A begins to saturate as well. This can be explained with the shape of the islands: once the volume of the truncated pyramids comes close to the pyramid volume, R_T is reduced and therefore the shrinkage of s_x too.

In the calculations, islands are counted as 3D islands once their height exceeds 3 ML's. This selection excludes quasi-3D islands of smaller height that are not formed strain driven but by direct hits from the vapor beam. The evolution of the 3D island density n_{3D} is shown in Fig. 4. Independent of the parameter set, n_{3D} increases abruptly at a certain coverage θ. This is in good accordance with our RHEED observations which at the critical coverage θ_C abruptly change from 2D to 3D patterns. In the following, we thus assume that the coverage, at which the calculated 3D island density increases, can be identified with θ_C.

After 20 s at $\theta = 2.0$ ML's deposition is stopped by switching off the flux $(F=0)$. In the calculations, the growth stop initiates a reduction of s_x and a strong increase of h_x (Fig. 4). To understand this behavior the following scenario is presented. During growth, there is a balance between mass transport to the island edges with rate R_A and removal of atoms with rate $R_D + R_T$. Both effects stabilize the size s of the island base area. When F is switched off, the rate R_A becomes negligible. Then $R_D + R_T$ is dominant and s shrinks as a consequence. On the other hand, the island volume does not shrink significantly from the above mechanism, and a nearly constant island volume at a smaller base area causes an increase of the island height. This result is very important and establishes that the shape of strain-induced 3D islands is not in equilibrium during growth.

In order to parametrize the growth model for InAs quantum dot formation on GaAs substrates, calculation results are compared to RHEED and AFM measurements. To avoid segregation of Ga from the substrate into the InAs film, the parametrization is performed at low growth temperatures of 420 °C, where intermixing is small[23] and thus $\delta = 7.26\%$. The flux is 0.1 ML/s. In a first step, the influence of the surface diffusion barrier E_{free} is studied. It is found that E_{free} is the central parameter for the island density n_{isl} in the 2D growth regime at low coverages. The influence of the other parameters on n_{isl} is small. Figure 5 shows calculated values of n_{isl} and s_x as function of E_{free} at a coverage $\theta = 1.0$ ML. The model parameters are chosen according to 2D growth via irreversible aggregation: $E_0 = 10$ eV, $c_B = 0$, and $c_U = 0$, where only E_{free} is important. Interestingly, $n_{isl} \sim (D/F)^{-1/3}$ as well as $s_x \sim (D/F)^{1/3}$ follow well-known scaling laws[22] for irreversible aggregation, despite the additional influence of the wetting layer in the present model. $D = \nu_{free}(a_0/2)^2$ is the surface diffusion coefficient. Furthermore, in the calculations we find a correlation between the total island density n_{isl} at $\theta = 1.0$ ML and the density n_{3D} of 3D islands at $\theta = 2.0$ ML's in the form $n_{isl}(\theta = 1.0\ \mathrm{ML}) \simeq n_{3D}(\theta = 2.0\ \mathrm{ML's})$. This allows us to compare the calculated only E_{free} dependent behavior of n_{isl} at $\theta = 1.0$ ML

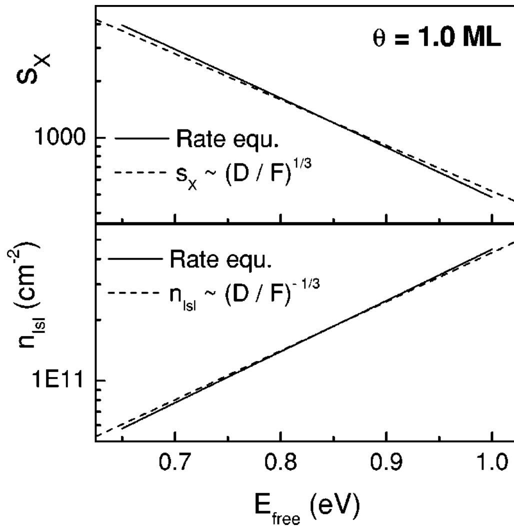

FIG. 5. Calculated s_x and n_{isl} at $\theta = 1.0$ ML as function of the surface diffusion barrier E_{free}. The model parameters $E_0 = 10$ eV, $c_B = c_U = 0$ are chosen according to irreversible aggregation of 2D islands. The dashed lines represent fits $s_x \sim (D/F)^{1/3}$ and $n_{isl} \sim (D/F)^{-1/3}$ in agreement with common scaling laws for irreversible aggregation. The growth parameters are $T = 420\,°\mathrm{C}$, $F = 0.1$ ML/s, and $\delta = 0\%$.

with AFM measurements of $n_{3D} \simeq 8 \times 10^{10}$ cm^{-2} for a sample grown at $T = 420\,°\mathrm{C}$, $F = 0.1$ ML/s, and $\theta = 2.0$ ML's, and thus the determination of $E_{free} = 0.70$ eV.

The spring model parameters are chosen with respect to the value of $\theta_C = 1.36$ ML's measured with RHEED at the above growth conditions. In the calculations, for a fixed $E_0 = 1.5$ eV, several combinations of c_B and c_U are found that result in the correct θ_C. On the other side, the ratio c_U / c_B strongly influences the island diameter shrinkage during the 2D to 3D transition and the resulting island height. This is demonstrated in Figs. 4 and 6. Parameter set A ($E_{free} = 0.70$ eV, $E_0 = 1.5$ eV, $c_B = 0.0304$, $c_U = 0.0176$) which accounts for strain in both the island base and in the bulk of the island is chosen for h_x ($\theta = 2.0$ ML's) $= 2.7$ nm under consideration of AFM measurements, where the island heights range from 2.5 to 3.0 nm. Parameter set B ($E_{free} = 0.70$ eV, $E_0 = 1.5$ eV, $c_B = 0.0484$, $c_U = 0$) describes a more simple growth model that reflects strain only in the island base. With the latter parameters we find h_x ($\theta = 2.0$ ML's) $= 1.5$ nm which is significantly lower than the experimental values. This is a clear proof for the importance of the strain in the bulk of the islands which enhances the mass transport on islands top and thus their height.

B. Critical coverage for quantum dot formation

In this section, the critical coverage θ_C is studied for variations of the growth parameters δ, F, and T. All following calculations are performed with the layer dependent strain model using parameter set A. In the first set of RHEED experiments, the influence of the lattice mismatch $\delta = (1 - x)(a_{InAs} - a_{GaAs})/a_{GaAs}$ is studied for different $In_{1-x}Ga_xAs$ samples. Variations of the GaAs growth speed

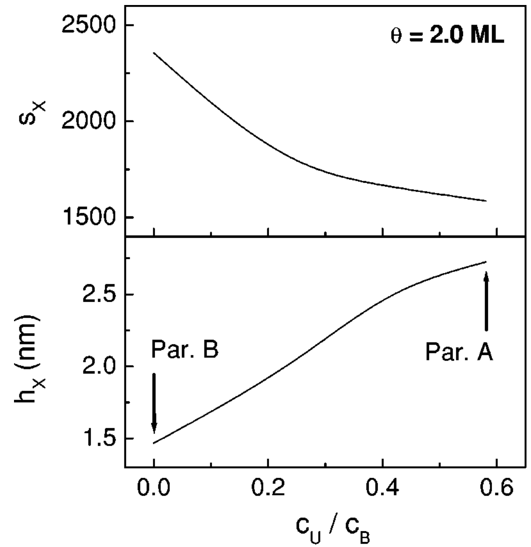

FIG. 6. Calculated s_x and h_x at $\theta = 2.0$ ML's dependent on the ratio c_U / c_B. All combinations of c_U and c_B shown here reproduce the experimental $\theta_C = 1.36$ ML's. The values that correspond to parameter sets A and B are marked by arrows.

$F_{GaAs} = 0.0$–0.23 ML/s at constant $F_{InAs} = 0.1$ ML/s yield $x = F_{GaAs}/(F_{GaAs} + F_{InAs}) = 0$–$70\%$. In the RHEED data, up to $x = 63\%$, θ_C increases significantly with decreasing δ which is obviously due to the reduced strain inside the growing film. For larger values of x, no 3D growth related features are observable in the RHEED spots even for very long deposition times. From this follows a minimal lattice mismatch necessary for 3D island formation of $\delta = 2.7\%$. As is demonstrated in Fig. 7, the calculations show a very good quantitative reproduction of the experimental data up to $x = 44\%$. This very important result establishes the applied two-spring approach as a suited approximation to describe the influence of strain during InGaAs quantum dot forma-

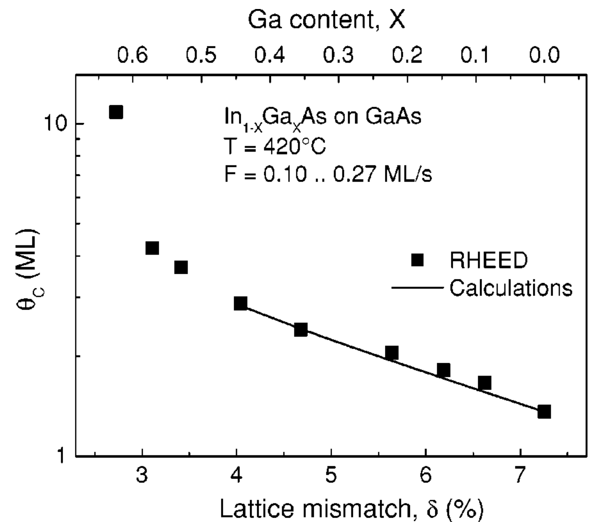

FIG. 7. Dependence of measured and calculated θ_C on the Ga content x during $In_{1-x}Ga_xAs$ deposition. The In flux of 0.1 ML/s is held constant and only the Ga flux is varied. Assuming homogeneous conditions, the lattice mismatch is calculated from x.

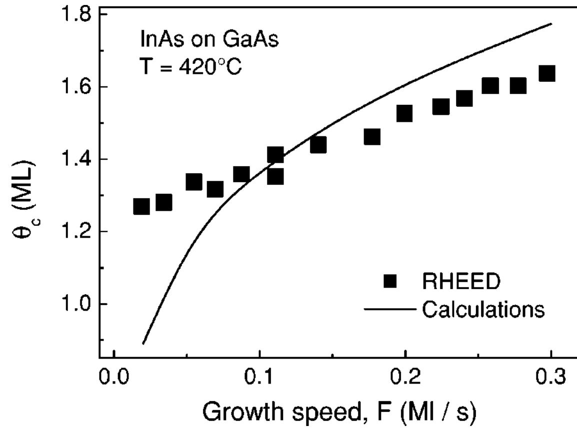

FIG. 8. Critical coverage θ_C for 2D to 3D transition as function of the growth speed. Plotted are RHEED measurements together with calculation results.

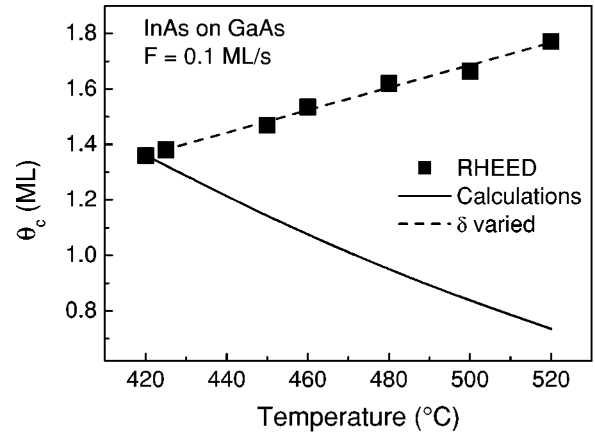

FIG. 9. Influence of the growth temperature on measured and calculated θ_C. The dashed line represents calculation results with adapted δ according to Fig. 10.

tion. At higher Ga contents, the RHEED measurements show intensity oscillations during the 2D growth regime that are associated with layer-by-layer growth. The wetting layer thickness determined from the number of oscillations lies beyond one monolayer and is thus not compatible with the geometrical assumptions of our model.

RHEED measurements of θ_C as function of F are shown in Fig. 8 together with calculation results. In the RHEED data we find a nearly linear increase of θ_C with F. The calculations show an increasing θ_C as well. In combination with the surface diffusion barrier the flux influences the island growth via the ratio (D/F). This is demonstrated by the scaling laws for n_{isl} and s_x discussed above. A higher flux means a higher density of mobile adatoms which will rather nucleate new islands instead of attaching to existing ones. Therefore an increase of F yields a higher density of smaller islands (Fig. 5). The critical lateral island size for formation of 3D islands is obtained later and θ_C is increased. The deviations of the calculation results from the RHEED data especially for small values of F are explained with the experimental procedure. In the experiments, only the In cell temperature is varied to set the flux, whereas the arsenic pressure is held constant. This results in a change of the III/V flux ratio, too, which is not considered in the growth model. For GaAs homoepitaxy, a high III/V ratio is expected to enhance the surface diffusion coefficient D.[24] This effect would counteract the flux in the measurements via (D/F) and reduce its influence on θ_C. Thus a smaller increase of θ_C would be expected in the calculated data, if the III/V flux ratio would be included in the model.

Variations of the growth temperature during InAs deposition point out an interesting behavior of θ_C (Fig. 9). We measure a nearly linear increase of θ_C with T which contradicts a simple thermally activated process. The rate equations yield a contrasting behavior where θ_C decreases with T. This qualitative disagreement indicates that the experimental data are affected by an additional mechanism that is not considered in the growth model. A very probable mechanism is an unintentional intermixing between gallium from the substrate and indium caused by temperature-dependent segregation during growth.[23] Assuming a homogeneous composition, the intermixing would result in strain reduction similar to the InGaAs growth experiments discussed above. In order to include this effect in the calculations, the effective lattice mismatch is adjusted such that the calculated θ_C agrees with the experimental value (dashed line in Fig. 9). In a next step the gallium content is calculated from this effective lattice mismatch. Figure 10 shows the such determined x values as function of the growth temperature. At 500 °C, we find a gallium content of 45%, that is in reasonable agreement with experiments[23] where a gallium content of about 30% is measured.

V. CONCLUSIONS

This paper presents a kinetic rate equation based model for the formation of quantum-dot-like islands in the Stranski-Krastanov mode. Quantitative agreement between the growth parameter dependence of the calculated critical coverage for 3D island formation and *in situ* RHEED experiments is demonstrated for variations of the lattice mismatch. The central

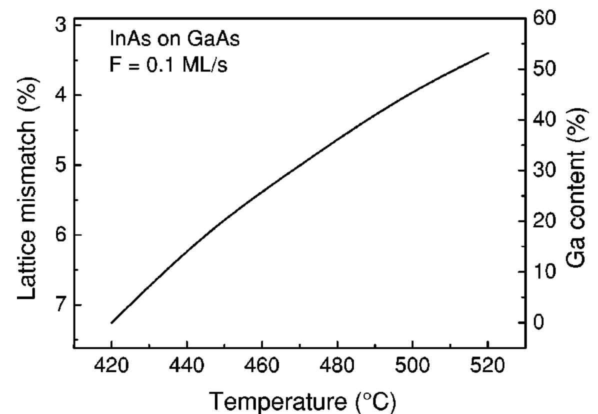

FIG. 10. Estimated temperature-dependent alloying due to Ga segregation into the InAs deposit. The respective Ga content is determined such that the resulting δ allows the reproduction of the RHEED data in Fig. 9.

point of this model is the inclusion of a layer dependent strain energy inside the growth islands. A direct consequence of this approach is the evolution of the calculated island size. Large 2D islands dominate the surface morphology at low coverages, whereas, during their transformation into 3D islands, the height increases and, importantly, the diameter shrinks. In this way enhanced mass transport on the island top at the expense of the island diameter is crucial for the spontaneous conversion from 2D to 3D islands. A simpler model which accounts only for the strain inside the island base layer yields a saturated island diameter without shrinkage and thus is not able to obtain realistic island heights.

A direct experimental verification of the shrinking island diameter was given by Kobayashi *et al.* using AFM measurements.[25] Furthermore, in the AFM data at $T = 500\,^{\circ}\mathrm{C}$ the critical coverage for the first observation of 3D islands is 1.57 ML's, which is close to $\theta_C = 1.68$ ML's determined here from RHEED measurements.

In an earlier publication by Koduvely and Zangwill,[12] a similar model has been used to describe 3D island evolution. However, there an only island diameter dependent strain energy was assumed. The island shape was derived from equilibrium energy minimization according to Tersoff and Tromp.[26] In order to calculate the coverage dependence of the island diameter, elastic interactions between islands had to be invoked that control atom detachment from 3D islands. When comparing their model to experiments, an unrealistic large value of the interaction parameter had to be assumed in order to reproduce the data.

Additional important consequences of the present model establish the significance of intermixing at higher temperatures as well as the nonequilibrium nature of the island size during growth. Since the shape and composition crucially determine the optical and electronical properties of these quantum dot islands, their control is essential for future applications and devices.

ACKNOWLEDGMENTS

The author would like to thank C. Dumat, S. Mendach, and W. Hansen for very helpful discussions, K. Zhang and C. Weichsel for the AFM measurements, S. Schnuell for keeping our MBE machine in good condition, Borland for Delphi V, and the ''Deutsche Forschungsgemeinschaft'' for support under SFB 508.

*FAX: 49 (0) 40 42838 6332; Email address: heyn@physnet.uni-hamburg.de

[1] D. Bimberg, M. Grundmann, and N. N. Ledentsov, *Quantum Dot Heterostructures* (John Wiley and Sons, Chichester, 1999).

[2] J.M. Moison, F. Houzay, F. Barthe, L. Lepronce, E. Andre, and O. Vatel, Appl. Phys. Lett. **64**, 196 (1994).

[3] A. Madhukar, Q. Xie, P. Chen, and A. Konkar, Appl. Phys. Lett. **64**, 2727 (1994).

[4] D. Leonard, M. Krishnamurthy, S. Fafard, J.L. Merz, and P.M. Petroff, J. Vac. Sci. Technol. B **12**, 1063 (1994); D. Leonard, S. Fafard, Y.H. Zhang, J.L. Merz, and P.M. Petroff, *ibid.* **12**, 2516 (1994).

[5] K. Mukai, N. Ohtsuka, M. Sugawara, and S. Yamazaki, Jpn. J. Appl. Phys., Part 2 **33**, L1710 (1994).

[6] J. Oshinowo, M. Nishioka, S. Ishida, and Y. Arakawa, Appl. Phys. Lett. **65**, 1421 (1994).

[7] A. Heinrichsdorff, A. Krost, M. Grundmann, D. Bimberg, A.O. Kosogov, and P. Werner, Appl. Phys. Lett. **68**, 3284 (1996).

[8] C. Priester and M. Lannoo, Phys. Rev. Lett. **75**, 93 (1995).

[9] N. Moll, M. Scheffler, and E. Pehlke, Phys. Rev. B **58**, 4566 (1998).

[10] H.T. Dobbs, D.D. Vvedensky, A. Zangwill, J. Johansson, N. Carlson, and W. Seifert, Phys. Rev. Lett. **79**, 897 (1997).

[11] B.A. Joyce, J.L. Sudijono, J.L. Belk, H. Yamaguchi, X.M. Zhang, H.T. Dobbs, A. Zangwill, D.D. Vvedensky, and T.S. Jones, Jpn. J. Appl. Phys., Part 1 **36**, 4111 (1997).

[12] H.M. Koduvely and A. Zangwill, Phys. Rev. B **60**, R2204 (1999).

[13] Ch. Heyn and C. Dumat, J. Cryst. Growth **227–228**, 990 (2001).

[14] Ch. Heyn, D. Endler, K. Zhang, and W. Hansen, J. Cryst. Growth **210**, 421 (2000).

[15] H. Lee, R. Lowe-Webb, W. Yang, and P.C. Sercel, Appl. Phys. Lett. **72**, 812 (1998).

[16] K. Zang, Ch. Heyn, W. Hansen, Th. Schmidt, and J. Falta, Appl. Phys. Lett. **76**, 2229 (2000).

[17] J. Marquez, L. Geelhaar, and K. Jacobi, Appl. Phys. Lett. **78**, 2309 (2001).

[18] Y. Chen and J. Washburn, Phys. Rev. Lett. **77**, 4046 (1996).

[19] G.S. Bales and D.C. Chrzan, Phys. Rev. B **50**, 6057 (1994).

[20] G.S. Bales and A. Zangwill, Phys. Rev. B **55**, R1973 (1997).

[21] Ch. Heyn, T. Franke, and R. Anton, J. Cryst. Growth **201/202**, 67 (1999).

[22] J.A. Venables, Philos. Mag. **27**, 693 (1973); J.A. Venables, G.D. Spiller, and M. Hanbücken, Rep. Prog. Phys. **47**, 399 (1984).

[23] P.B. Joyce, T.J. Krzyzewski, G.R. Bell, B.A. Joyce, and T.S. Jones, Phys. Rev. B **58**, R15 981 (1998).

[24] Ch. Heyn and M. Harsdorff, Phys. Rev. B **55**, 7034 (1997). Ch. Heyn, T. Franke, and R. Anton, *ibid.* **56**, 13 483 (1997).

[25] N.P. Kobayashi, T.R. Ramachandran, P. Chen, and A. Madhukar, Appl. Phys. Lett. **68**, 3299 (1996).

[26] J. Tersoff and R.M. Tromp, Phys. Rev. Lett. **70**, 2782 (1993).